Journal of Cellular Biochemistry 98:810–826 (2006)

Quantitative Analysis of Localization and Nuclear Aggregate Formation Induced by GFP-Lamin A Mutant Proteins in Living HeLa Cells

S. Hübner,* J.E. Eam, K.M. Wagstaff, and D.A. Jans

Nuclear Signaling Laboratory, Department of Biochemistry and Molecular Biology, PO Box 13D, Monash University, Clayton, Victoria 3800, Australia

Abstract Although A-type lamins are ubiquitously expressed, their role in the tissue-specificity of human laminopathies remains enigmatic. In this study, we generate a series of transfection constructs encoding missense lamin A mutant proteins fused to green fluorescent protein and investigate their subnuclear localization using quantitative live cell imaging. The mutant constructs used included the laminopathy-inducing lamin A rod domain mutants N195K, E358K, M371K, R386K, the tail domain mutants G465D, R482L, and R527P, and the Hutchinson–Gilford progeria syndrome-causing deletion mutant, progerin (LaAΔ50). All mutant derivatives induced nuclear aggregates, except for progerin, which caused a more lobulated phenotype of the nucleus. Quantitative analysis revealed that the frequency of nuclear aggregate formation was significantly higher (two to four times) for the mutants compared to the wild type, although the level of lamin fusion proteins within nuclear aggregates was not. The distribution of endogenous A-type lamins was altered by overexpression of the lamin A mutants, coexpression experiments revealing that aberrant localization of the N195K and R386K mutants had no effect on the subnuclear distribution of histones H2A or H2B, or on nuclear accumulation of H2A overexpressed as a DsRed2 fusion protein. The GFP-lamin fusion protein-expressing constructs will have important applications in the future, enabling live cell imaging of nuclear processes involving lamins and how this may relate to the pathogenesis of laminopathies. J. Cell. Biochem. 98: 810–826, 2006.

Key words: lamin A; laminopathy; intermediate filaments; nuclear aggregates; nuclear envelope; HGPS

The nucleus is a defining feature of the eukaryotic cell, being integrally involved in cellular signaling processes. Nuclear integrity is preserved through a nucleoskeletal filament system formed largely by members of the lamin family of nuclear localizing intermediate filaments (IF). Lamins form a fibrous proteinaceous structure, 20–50 nm in diameter, which underlies the inner nuclear membrane (INM) of the nuclear envelope (NE) and interacts with a number of INM integral proteins. In addition to their localization at the nuclear periphery, lamins are also present in the nucleoplasm, where A-type lamins in particular are believed to play important roles in nuclear processes.

Nuclear lamins, like cytoplasmic IF proteins, contain a central α-helical rod domain, flanked by non-α-helical "head" and "tail" domains. Lamins can be classified into the developmentally expressed A-type and the constitutively expressed B-type lamins. Mammalian cells express four A-type lamins (lamin A, AΔ10, C and C2) from one gene (*LMNA*) by alternative splicing and three B-type lamins (lamin B1, B2, and B3) encoded by two genes (*LMNB1* and *LMNB2*). Lamin A, but not lamin C, contains a terminal tetrapeptide sequence, the CaaX motif (C, cysteine, a, aliphatic, X, any amino acid), which is the site of post-translational farnesylation. B-type lamins, which also contain a CaaX motif, are constitutively farnesylated [Beck et al., 1990; Sinensky et al., 1994a], whereas lamin A carries this modification only

Grant sponsor: NHMRC; Grant number: 143710, 334013.

Dr. S. Hübner's present address is Institute of Anatomy and Cell Biology, University of Würzburg, Koellikerstrasse 6, 97070 Würzburg, Germany.

*Correspondence to: Dr. S. Hübner, Nuclear Signaling Laboratory, Department of Biochemistry and Molecular Biology, PO Box 13D, Monash University 3800, Australia. E-mail: stefan.huebner@mail.uni-wuerzburg.de

Received 14 June 2005; Accepted 18 November 2005

DOI 10.1002/jcb.20791

temporarily and soon after its incorporation into the filament system, the farnesyl group is removed in a multi-step process [Weber et al., 1989]. The globular tail domain of lamins includes an evolutionarily conserved domain containing an immunoglobulin-like fold comprising a pair of β-sheets [Dhe-Paganon et al., 2002; Krimm et al., 2002], within which many disease-causing mutations reside.

A group of heritable human diseases, known as laminopathies, have been identified over the last ~10 years, mostly associated with mutations in *LMNA*. Based on tissue-specificity and clinical phenotypes, laminopathies can be broadly grouped into distinct categories, with prominent features of muscular dystrophy, lipodystrophy and neuropathy, while other laminopathies display a rather complex clinical phenotype with more pleiotropic effects on development (see www.ncbi.nlm.nih.gov/entrez/query.fcgi? CMD = search&DB = omim).

Opposing structural and gene expression hypotheses have been proposed to explain why mutations within *LMNA* give rise to distinct diseases. As the lamina is an essential determinant of nuclear shape and stability [Newport et al., 1990; Lenz-Bohme et al., 1997; Sullivan et al., 1999; Liu et al., 2000], structural defects within it may contribute to pathology. This is consistent with the observation that skin fibroblasts from autosomal dominant Emery–Dreifuss muscular dystrophy (AD-EDMD—[Bonne et al., 1999]) patients or *LMNA* knockout fibroblasts display increased nuclear fragility [Markiewicz et al., 2002b; Broers et al., 2004; Lammerding et al., 2004]. The alternative hypothesis proposes that the nuclear lamina may play a role in tissue-specific gene expression. As lamins and other NE proteins directly or indirectly bind to DNA and heterochromatin/histones, this interaction could contribute to the spatial localization of chromatin within the cell nucleus. Thus, alterations of the nuclear lamina organization through loss of A-type lamin function could lead to changes in chromatin distribution [Liu et al., 2000; Vigouroux et al., 2001; Favreau et al., 2003; Nikolova et al., 2004] and possibly gene expression. In addition, A-type lamins have also been proposed to interact with key transcriptional regulators such as the retinoblastoma protein [Ozaki et al., 1994; Markiewicz et al., 2002a; Hübner et al., 2005], members of the sterol responsive element binding protein (SREBP) family [Lloyd et al., 2002; Hübner et al., 2005] and MOK2 [Dreuillet et al., 2002].

The impact of pathogenic A-type lamin expression on the subnuclear localization of A-type lamin-binding proteins, NE-structure and nuclear function have been investigated using either cultured skin fibroblasts obtained from laminopathy patients [Vigouroux et al., 2001; Favreau et al., 2003], or cultured cell lines ectopically expressing FLAG- or HA-tagged A-type lamin fusion proteins [Holt et al., 2001; Ostlund et al., 2001; Raharjo et al., 2001; Bechert et al., 2003; Favreau et al., 2003; Sebillon et al., 2003], where cells were fixed and permeabilized to enable visualization of overexpressed proteins by immunostaining. With few exceptions [Gilchrist et al., 2004; Broers et al., 2005], live cell imaging with respect to the study of lamins carrying laminopathy-inducing mutations has largely been lacking.

To begin to address this shortfall, the present study uses GFP as a fusion tag to study lamin A dynamics, enabling investigation of the subnuclear localization of pathogenic lamin A proteins in living cells. We show that, with the exception of the deletion mutant progerin, all of the mutants, as well as wild type lamin A, can induce nuclear aggregates, although the mutants show a two- to four-fold higher frequency of aggregate formation. There were no significant differences between the proteins in terms of their concentration within nuclear aggregates, however. Aggregate formation also disrupted endogenous lamina organization, but had no effect on either intranuclear localization or nuclear accumulation of coexpressed core histones. Of all of the mutants, progerin uniquely was found to increase lobulation of the NE. The GFP-lamin A fusion proteins will have important application in analyzing the effects of lamin A mutant expression on nuclear processes in living cells.

MATERIALS AND METHODS

Plasmid Construction

To derive constructs for the expression of pathogenic human pre-lamin A proteins in mammalian cells, expression vector pSVK3, provided by H.J. Worman (Departments of Medicine and of Anatomy and Cell Biology, Columbia University, New York, USA), was digested with restriction endonucleases XhoI

and BamHI and the wild type pre-lamin A cDNA ligated into the similarily digested entry vector pENTR11 (Invitrogen, Life Technologies). The resultant pENTR11 pre-lamin A was subsequently digested with BstEII to delete the coding sequence for pre-lamin A amino acids 124–641 and then ligated with BstEII-generated pre-lamin A cDNA fragments from the pSVK3- and pCS2 + pre-lamin A vectors, which encode the pathogenic pre-lamin A proteins N195K, E358K, M371K, and R386K (also provided by H.J. Worman), and G465D, R482L, and R527P (provided by M. Osborn, Max Planck Institute for Biophysical Chemistry, Göttingen, Germany). The pre-lamin A wild type and mutant cDNAs were ultimately transferred into destination vector pDEST53 encoding GFP-fusion proteins under control of the CMV promotor by site-specific recombination, using Gateway™ technology (Invitrogen, Life Technologies). Destination clone DsRed2-LaA was obtained by recombination between pENTR11-pre-lamin A and Gateway compatible DsRed2 plasmid [Soboleva et al., 2005].

A Gateway™-compatible LaAΔ50-cDNA was generated by high fidelity PCR using primers containing the attB1 and attB2 recombination sites and the expression vector pSVK3 pre-lamin A as a template. The primers used were attB1LaAΔ50 (5′-GGGGACAAGTTTGTACAAAAAAG CAGGCTGTGAGACCCCGTCCCAGC-3′) and attB2LaAΔ50 (5′-GGGGACCACTTTGTACAAGAAAGCTGGGTTATTACATGATGCTGCAGTTCTGGGGGGCTCTGGGCTCCTGAGCCGC-3′) where the human pre-lamin A-specific nucleotides are underlined. Use of primer attB2LaAΔ50 enabled the deletion of a 150 nucleotide sequence (nucleotides 1819–1968) at the C-terminus of the human pre-lamin A cDNA. The amplified LaAΔ50-cDNA fragment was first transferred into entry vector pDONR207 (Invitrogen, Life Technologies), generating entry clone pDONR207-LaAΔ50, and then into destination vector pDEST53 (Invitrogen, Life Technologies) by recombinational cloning. Destination clone pEPI-LaAΔ50 was obtained by recombinational cloning between entry clone pDONR207-LaAΔ50 and pEPI, previously made Gateway™ compatible, using the Gateway™ Vector Conversion kit (Invitrogen, Life Technologies), according to manufacturer's instructions [Ghildyal et al., 2005]. pEPI is a pEGFPC1-derived episomally replicating expression vector, which allows long-term expression of encoded proteins [Piechaczek et al., 1999]. The cDNA fragments in pENTR11 pre-lamin A and pDONR207-LaAΔ50 were verified by automated DNA sequencing.

To generate plasmids pDsRed2-H2A and pDsRed2-H2B, the coding sequences of *Xenopus* histones H2A and H2B were generated by PCR using the primers 5′-GGGGACAAGTTTGTACAAAAAAGCAGGCTTCATGTCAGGAACAGG-CAAACAAG-3′ and 5′-GGGGACCACTTTGTACAAGAAAGCTGGGTCCTTGCTCTTGGCAG-ATTTGGC-3′ (H2A) and (5′-GGGGACAAGTTTTACAAAAAAGCAGGAGGCTTGGATATCC-CTGAGCCCGCC-3′ and 5′-GGGGACACTTTGTACAAGAAAGCTGGGTCTAGGCGCTGGT-GTACTTGGTGCG-3′ (H2B) using high fidelity PCR and the vectors pET5a-H2A and pET5a-H2B as templates. These were subsequently transferred into pDONR207 using homologous recombination (Gateway™ Technology) resulting in the pDONR207-H2A and pDONR207-H2B vectors. The coding sequences were then transferred by recombination into the destination vector pBk-CMV-DsRed2 (DsRed2 coding sequence expressed from the CMV promoter in pBk-CMV), which was made Gateway™ compatible using the Gateway™ Vector Conversion kit according to the manufacturer's instructions. The fidelity of all constructs was verified by DNA sequencing.

Cell Culture and Transfection

Human cervical adenocarcinoma HeLa cells and mouse C2C12 myoblasts were cultured in Dulbecco's modified Eagle's medium (DMEM) supplemented with 10% heat-inactivated fetal calf serum (FCS), penicillin, and streptomycin in a humidified 37°C incubator with 5% CO_2. Transfection was performed using lipofectAMINE 2000 (Invitrogen, Life Technologies). One day before transfection, HeLa and C2C12 cells were seeded on to 15 × 15 mm coverslips in 12-well culture plates or 18 mm diameter round coverslips in six-well culture plates (for live cell imaging) and grown for 16–24 h to 50%–70% confluence. For transfection, 2 μg plasmid DNA was mixed with serum-free DMEM in a total volume of 50 μl, which was added to 50 μl containing lipofectAMINE 2000 diluted 1:25 in serum free DMEM and incubated for 20 min at room temperature. This mixture was then added directly to the cells, which were then returned to the incubator. Cotransfection of

HeLa cells was carried out using TransIT-LT1 (Mirus Corporation). Three microliters of Trans-IT-LT1 were mixed with 50 μl serum free DMEM and incubated for 20 min at room temperature. Two micrograms DNA (1 μg of each construct) was then added to the mixture, incubated for 20 min at room temperature, and the mixture added to the cells, which were then returned to the incubator.

Confocal Laser Scanning Microscopy (CLSM)/Image Analysis

Transfected cells were analyzed by CLSM with equatorial images derived using a Perkin Elmer Ultraview live cell imaging system, equipped with a reverse 100× oil immersion objective (Olympus). For live imaging, cells were maintained in phenol red-free DMEM medium in a coverslip chamber and the imaging performed using a 37°C-heated stage. Images were also collected through the entire cell to produce a z-series that was used to generate a projection image of the nucleus. Images obtained by CLSM were analyzed using the ImageJ 1.62 public domain software, as previously [Forwood and Jans, 2002]. The mean nuclear (Fn) and cytoplasmic (Fc) fluorescence were quantified to enable the nuclear to cytoplasmic ratio (Fn/c) to be determined according to the formula: $Fn/c = (Fn-Fb)/Fc-Fb)$, where Fb is the mean background fluorescence (autofluorescence). Quantitation of the mean fluorescence of lamin A nuclear aggregates (Fn_a) was determined according to the formula: $Fn_a = Fn_a-Fb$. Statistical analysis was performed using the Student's *t*-test (unpaired, two-tailed—InStat 2.01 software package) as previously [Hu and Jans, 1999].

Immunofluorescence

Transfected cells grown on coverslips were washed with PBS and fixed and permeabilized with either methanol/acetone (1:1, −20°C) for 10 min at −20°C or 4% para-formaldehyde for 10 min, and Triton X-100 (0.05%) for 5 min. Following washes with PBS, the fixed cells were blocked for 1 h with 2% BSA/0.05% Tween 20 at room temperature and then incubated with either monoclonal anti-lamin A/C (Imgenex, IMG 703-4; 1:1,000) or monoclonal anti-FLAGM2 (Sigma-Aldrich, Deisenhofen, Germany: 1:1,000) for 3 h at 4°C. After 3 washes with PBS/0.05% Tween 20, cells were incubated for 1 h at 4°C with the Alexa Fluoro-568-conjugated goat anti-mouse secondary antibody (1:1,000). Cells were finally washed with PBS/0.05% Tween 20 and mounted.

RESULTS

Subnuclear Localization of GFP-Lamin A Mutant Proteins

To determine the subnuclear localization of pathogenic lamin A mutants expressed as GFP-fusion proteins, we generated a series of expression vectors encoding the lamin A mutants: N195K, found in patients with dilated cardiomyopathy (DCM) [Fatkin et al., 1999]; E358K, M371K, R386K, and R527P, identified in patients with AD-EDMD [Bonne et al., 1999; Bonne et al., 2000]; G465D and R482L, found in patients with familial partial lipodystrophy (FPLD) [Cao and Hegele, 2000; Shackleton et al., 2000], and LaAΔ50 found in patients with Hutchinson–Gilford progeria syndrome (HGPS) [Cao and Hegele, 2003; De Sandre-Giovannoli et al., 2003; Eriksson et al., 2003] (see Fig. 1). The expression constructs encode the precursor form of lamin A, pre-lamin A, which is subsequently processed by a two-step endoproteolytic cleavage of the final 18 amino acids [Weber et al., 1989; Sinensky et al., 1994b]. Transfection efficiencies for the different constructs and the level of expression of the respective lamin A wild type and mutant GFP-fusion proteins in HeLa cells were comparable in all cases (not shown). Figure 2A displays the representative subnuclear localization pattern 16–24 h post transfection of the GFP-lamin A fusion proteins used in this study in living, transfected HeLa cells. Immunoblot analysis of cell lysates revealed proteins of the anticipated sizes (not shown). The formation of nuclear aggregates was the most dramatic nuclear phenoytype seen upon overexpression of wild type and mutant proteins (see summary in Table I). In cells transfected to express GFP-lamin A (GFP-LaA), the majority of cells showed a uniform to near uniform localization of GFP-LaA at the nuclear periphery, indicating incorporation of GFP-LaA into the nuclear lamina (Fig. 2A a, a′, and b). In a subset of transfected cells (17%), mislocalization into nuclear aggregates could also be observed (Fig. 2A c), but the majority of such cells contained nuclei with only few, and generally small aggregates. Nuclear aggregate formation was also detected in non-transfected HeLa cells immunostained for

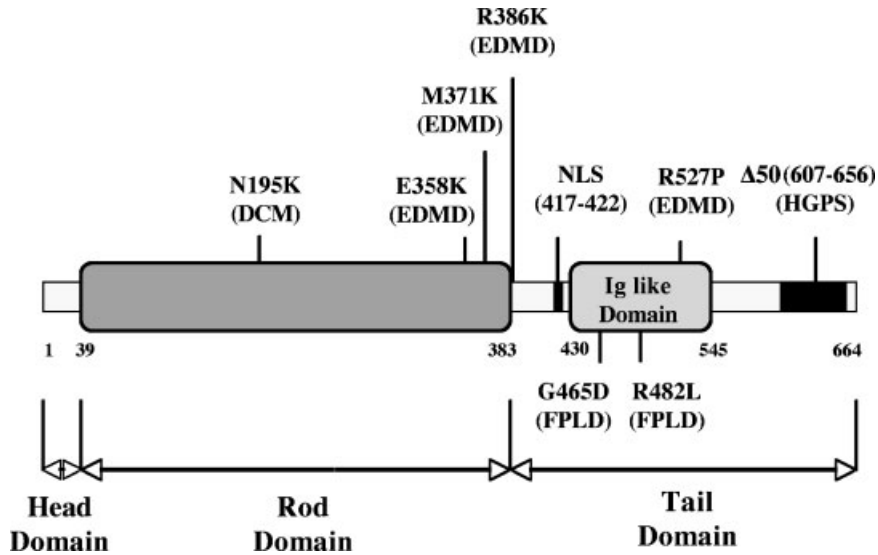

Fig. 1. Domain structure of pre-lamin A, indicating the positions of the pathogenic mutations used in this study, together with the associated diseases. DCM, dilated cardiomyopathy; EDMD, Emery–Dreyfuss muscular dystrophy; FPLD, familal partial lipodystrophy; HGPS, Hutchinson–Gilford progeria syndrome; NLS, nuclear localization signal.

endogenous lamin A/C (not shown). Such subnuclear localization of wildtype lamin A has previously been reported and found to correspond to functionally distinct types of intranuclear structures [Bridger et al., 1993; Moir et al., 1994; Hozak et al., 1995; Machiels et al., 1995; Sasseville and Raymond, 1995; Pugh et al., 1997; Spann et al., 1997; Jagatheesan et al., 1999; Neri et al., 1999; Kennedy et al., 2000; Muralikrishna et al., 2004]. However, the intranuclear, endogenous lamin-containing foci appear to be distinct from lamin A-mutant induced aggregates [Capanni et al., 2003]. GFP-LaA was also detected in the cytoplasm within perinuclear structures (not shown). This property, which has not been previously reported, was also observed in all of the lamin A mutant expressing cells, and is presumably a result of overexpression.

In cells expressing the rod domain mutant GFP-LaAE358K, the majority of transfected cells displayed discontinous lamina fluorescence (Fig. 2A g and g′), with 40% additionally containing nuclear aggregates (Fig. 2A h), whereas cells with nuclei containing aggregates only, that is, without any rim fluorescence, were rarely observed. Similar observations have been reported for HA-tagged lamin A mutant proteins R453W and R482W [Favreau et al., 2003]. In some cells, nuclei with continous lamina fluorescence were also detectable (Fig. 2A i). The number of aggregates per nucleus in GFP-LaAE358K-expressing cells was lower than in the other rod domain lamin A mutants (N195K, M371K, and R386K see below), with the lowest frequency of cells showing nuclear aggregate formation. HeLa cells expressing GFP-LaAN 195K and GFP-LaAM371K showed a mainly nuclear aggregate-only phenotype (Fig. 2A d, d′, and j, j′), generally with numerous aggregates, larger than those seen in either GFP-LaAE 358K- or GFP-LaA-expressing cells. Additionally, cells could be detected with very large aggregates, resembling those seen in Figure 2A m and m′. Other transfected cells displayed discontinous lamina fluorescence (Fig. 2A e and k) similar to that of the E358K mutant, either with or without additional nuclear aggregates. In low expressing cells, diffuse and weak NE localization of GFP-LaAN195K (Fig. 2A f) and GFP-LaAM371K (not shown) was detectable. The majority of cells expressing GFP-LaAN 195K and GFP-LaAM371K at low levels, however, contained nuclei with few aggregates, indicating that the N195K and M371K mutations impair lamina assembly more than the E358K mutant. In GFP-LaAE358K- but not in GFP-LaAN195K-expressing cells, continuous fluorescent nuclear lamina could be detected (Fig. 2A i). Seventy-one percent and 76% of transfected cells showed nuclei with aggregates in the case of cells expressing N195K and

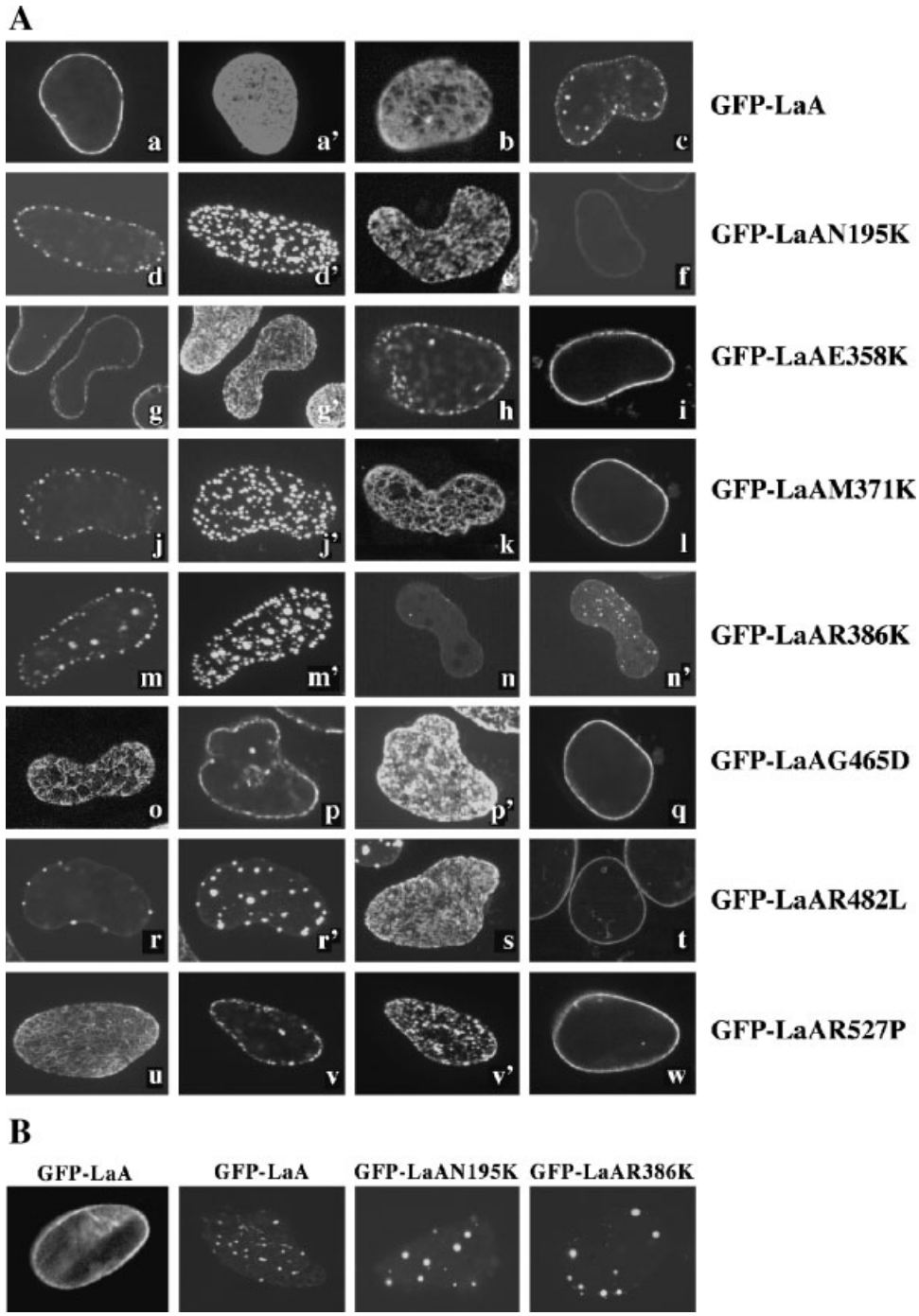

Fig. 2. Normal and aberrant localization of overexpressed disease-causing GFP-lamin A fusion proteins in cultured cells. CLSM images of live HeLa (**A**) and C2C12 (**B**) cells expressing wild type and mutant GFP-lamin A fusion proteins performed 16–24 h post transfection. A: CLSM images display individual nuclei with mislocalizing GFP-lamin A fusion proteins. Images on the left most panel represent the most prominent nuclear phenotype. Z-series of x–y images through the entire volume of the nucleus were additionally generated, and the images subsequently combined and converted into projection images (a′, d′, g′, j′, m′, n′, p′, r′, v′). Juxta-equatorial scanning through the nucleus was also performed to display discontinous lamina fluorescence (b, e, k, o, s, u). B: CLSM images display representative aggregate-containing individual nuclei in C2C12 cells expressing the indicated wild type and mutant GFP-lamin A fusion proteins.

TABLE I. Summary of Nuclear/Intranuclear Localization of GFP-Lamin A Constructs and Frequency of Nuclear Aggregate Formation in Transfected HeLa Cells

GFP-fusion protein expressed	GFP-lamin A localization[a]	% Cells with aggregates (n)[b]
GFP-LaA[c]	Continuous NE-fluorescence > discontinuous NE-fluorescence with/without aggregates	17 (1273)
GFP-LaN195K[c]	Aggregates only > discontinuous NE-fluorescence with/without aggregates	76 (822)
GFP-LaE358K[c]	Discontinuous NE-fluorescence with/without aggregates > aggregates only > continuous NE-fluorescence	40 (1027)
GFP-LaM371K	Aggregates only > discontinuous NE-fluorescence with/without aggregates > continuous NE-fluorescence	71 (947)
GFP-LaR386K	Aggregates only	73 (1175)
GFP-LaG465D	Discontinuous NE-fluorescence with/without aggregates > continuous NE-fluorescence	31 (973)
GFP-LaR482L	Aggregates only > discontinuous NE-fluorescence with/without aggregates > continuous NE-fluorescence	72 (962)
GFP-LaR527P	Discontinuous NE-fluorescence with/without aggregates > continuous NE-fluorescence	33 (881)

[a]The GFP-lamin A phenotypes are listed in order of frequency; see representative images in Figure 2. Nuclear aggregate formation was the most overt phenotype. NE, nuclear envelope.
[b]Percentage of cells containing nuclear aggregates 24 h post transfection. Results are pooled from three independent experiments. In all cases, significant differences ($P < 0.05$) were observed between the number of nuclear aggregates in mutant versus wild type lamin A-expressing cells.
[c]Expression of GFP-LaA, GFP-LaAN195K, and GFP-LaAR386K was also conducted in the laminopathy-relevant cell line C2C12. Nuclear aggregate formation occurred at similar frequencies as in HeLa cells, with 18.5% of GFP-LaA-expressing cells containing nuclear aggregates, and a much higher frequency of nuclear aggregates in GFP-LaAN195K- and GFP-LaAR386K-expressing cells (78.1% and 82.5%, respectively).

M371K lamin A mutants, the mutations in the rod domain thus resulting in severe lamin assembly defects. The most assembly incompetent rod domain mutant, however, appeared to be R386K, where 72% of transfected cells showed nuclear aggregates regardless of the expression level (Fig. 2A m, m′, and n, n′). Continuous lamina fluorescence was rarely detected. Generally, nuclear aggregates were numerous and of similar size to those formed by GFP-LaAN195K and GFP-LaAM371K, but with a greater tendency to form large aggregates (see Fig. 2 m and m′).

Experiments with GFP-LaA and the myopathy-causing GFP-LaAN195K and -LaAR386K mutants were similarly conducted in the more laminopathy-relevant C2C12 cell line (see Fig. 2B). As in HeLa cells, aggregates were induced in GFP-LaA-expressing C2C12 cells, but they were generally smaller than the aggregates induced upon expression of GFP-LaAN195K or GFP-LaAR386K. The frequency of aggregate formation of the lamin A fusion proteins was comparable to that in HeLa cells, with 18.5% of cells containing nuclear aggregates after ectopic expression of GFP-LaA, and 78.1% and 82.5% respectively after expression of GFP-LaAN195K and GFP-LaAR386K (Table I). In short, no significant differences could be discerned between the two cell lines.

Lamin A mutants known to form nuclear aggregates due to point mutations within the Ig-fold of the tail domain (G465D, R482L, and R527P) were also examined in HeLa cells. G465 and R482 are clustered within the Ig-fold, with R482 being a hot spot for mutations, while R527 is found in a completely different location. Intriguingly a total of three different substitutions have now been documented at amino acid position 482 that lead to laminopathies with different tissue involvement. The strongest induction of nuclear aggregates among these mutants was observed for GFP-LaAR482L (72%) (Fig. 2A r and r′), while cells expressing GFP-LaAG465D, and GFP-LaAR527P showed a lower frequency of nuclear aggregate formation (31% and 33% respectively) (Table I, Fig. 2A o, o′, and u, u′). GFP-LaAG465D and GFP-LaAR527P-expressing cells were most dissimilar to cells expressing GFP-LaA, with the majority of nuclei exhibiting discontinous lamina fluorescence (Fig. 2A s and v), followed by nuclei showing both discontinous lamina and nuclear aggregates. The aggregates were similar in size to those seen in nuclei containing rod-domain mutants, with large aggregates rarely evident. Continuous lamina fluorescence was detectable but was significantly less frequent compared to cells expressing GFP-LaA (Fig. 2A t and w). The expression of the tail mutant GFP-LaAR482L resulted in a lamina phenotype very

similar to that seen in cells expressing GFP-LaAN195K, GFP-LaAM371K, and GFP-LaAR 386K. Seventy-two percent of cells had nuclei containing numerous nuclear aggregates either with or without discontinous lamina fluorescence (Fig. 2A s). Continuous lamina fluorescence was rarely seen (Fig. 2A t). These findings are consistent with previous reports [Bechert et al., 2003] that the R482L mutation results in the most assembly incompetent lamina phenotype, with the highest frequency of nuclear aggregate formation compared to other tail domain mutants. A summary of the nuclear phenotypes, as well as statistical analysis of nuclear aggregate formation upon expression of GFP-lamin A constructs is shown in Table I.

Immunofluorescence analysis of HeLa cells transfected with constructs encoding the GFP-lamin A mutants N195K and R386K revealed colocalization of endogenous A-type lamins within nuclear aggregates and disruption of the lamina lattice structure (Fig. 3b,c). In the absence of any nuclear aggregate formation, the endogenous lamin lattice displayed homogeneous rim fluorescence (Fig. 3a). The results thus indicate that the lamin A mutant proteins can interfere with the targeting and assembly of endogenous A-type lamins [Ostlund et al., 2001; Raharjo et al., 2001]; this may represent part of the basis of pathology in laminopathy patients.

Quantitative Analysis of Nuclear Aggregates Formed by GFP Lamin A Mutant Proteins

To investigate whether there were mutant-specific differences in the concentration of wild type opposed to mutant lamin A proteins within nuclear aggregates, the mean fluorescence intensity of aggregates (Fn_a) was quantitated in living C2C12 myoblasts, expressing GFP-LaA or the rod domain lamin A mutants GFP-LaAN195K, GFP-LaAE358K, GFP-LaAM371K, and GFP-LaAR386K. The mean fluorescence intensities were determined as described in Materials and Methods with the specific Fn_a values obtained from lamin A wild type aggregates ($Fn_a = 1$) compared to those obtained from lamin A mutant aggregates. The results revealed that the relative intensity of aggregate fluorescence for all rod domain mutants in C2C12 myoblasts was very similar to that of GFP-LaA, with relative Fn_a values of 0.81 for GFP-LaAN195K, 0.81 for GFPLaAM371K and 0.96 for GFP-LaAR386K (see Table II). Only GFP-LaAE358K seemed to have a lower relative aggregate fluorescence intensity (Fn_a of 0.61).

Expression of GFP-LaAΔ50 Induces a Dysmorphic Nuclear Phenotype

Subnuclear localization studies were also conducted for an expression construct encoding the HGPS-causing deletion mutant, progerin (LaAΔ50). This mutant is most commonly caused by a de novo heterozygous silent substitution at codon 608 (G608G) of the *LMNA* gene that ultimately leads to the in-frame deletion of 50 amino acids within the tail domain. This aberrant splicing event deletes the second endoproteolytic site, resulting in incomplete maturation of the lamin A precursor molecule. Transfection of HeLa cells with the pEPI-LaAΔ50 and the pEPI-LaA expression plasmids revealed that a significantly higher proportion of cells expressing GFP-LaAΔ50 possess nuclei with a dysmorphic, lobulated shape (33%, n = 1285–Fig. 4b,c) than GFP-LaA expressing cells (16%, n = 1283). However, the majority of transfected cells were indistinguishable from wild type lamin A expressing cells in terms of nuclear rim fluorescence (Fig. 4a). Analogous experiments conducted using pDEST53-based expression vectors (which result in lower protein expression levels—not shown) yielded similar results, although the percentage of dysmorphic nuclei was lower, with only 23.3% (n = 313) of the GFP-LaAΔ50 expressing cells displaying a lobulated phenotype compared to 16.5% (n = 212) of cells expressing GFP-LaA. We also observed that nuclear aggregate formation in GFP-LaAΔ50 expressing HeLa cells was significantly lower (2%, n = 600) compared to cells expressing the wild type form of lamin A (17%, n = 1273). In addition to nuclear rim fluorescence, perinuclear fluorescence could be observed in cells expressing high levels of GFP-LaAΔ50 (not shown).

In order to investigate whether expression of FLAG-LaAN195K increases nuclear aggregation of GFP-LaAΔ50, HeLa cells were cotransfected with constructs encoding GFP-LaAΔ50 and FLAG-LaAN195K. In all double-transfected cells, colocalization of FLAG-LaAN195K and GFP-LaAΔ50 in nuclear aggregates could be detected, indicative of an interaction between the two mutant proteins and recruitment of GFP-LaAΔ50 into FLAG-LaAN195K-generated aggregates (Fig. 4d–f). Thus, although

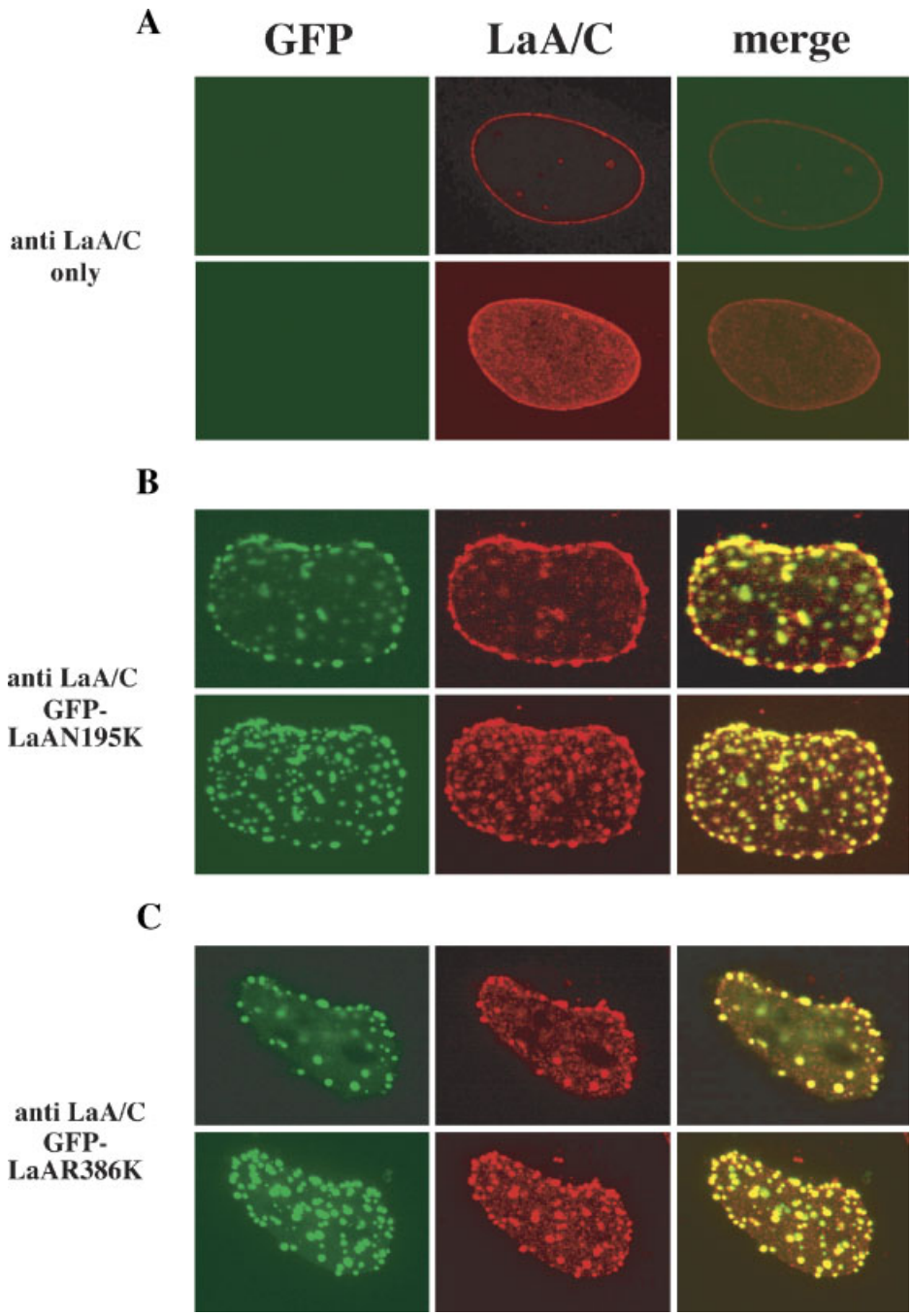

Fig. 3. Disruption of endogenous A-type lamins upon overexpression of GFP-lamin A mutants. CLSM images of overexpressed GFP-lamin A mutants and endogenous A-type lamins in HeLa cells 24 h post transfection. Endogenous A-type lamins were visualized after immunostaining of methanol/acetone fixed cells with a monoclonal anti A-type lamin antibody and an Alexa 568-coupled secondary antibody (**middle panels**). Panels depict nontransfected cells (**A**) or cells overexpressing GFP-LaAN195K (**B**) or GFP-LaAR386K (**C**). Images on the left represent the GFP-fusion proteins, images in the middle represent the anti-A-type lamin immunostaining and images on the right represent the merged images, where yellow coloration is indicative of colocalization. The **upper panels** in each of A–C depict images with an equatorial slice through the cell, whereas the **bottom panels** depict projection images. [Color figure can be viewed in the online issue, which is available at www.interscience.wiley.com.]

LaAΔ50 itself does not appear to induce nuclear aggregates (but rather has other effects on nuclear morphology), the LaAN195K mutant appears to be dominant in terms of recruiting LaAΔ50 into nuclear aggregates. Colocalization of FLAG-LaAN195K and GFP-LaAΔ50 within perinuclear structures was also frequently observed. Although the significance is not clear,

TABLE II. Quantitative Analysis of Nuclear Aggregates Induced in Mouse C2C12 Myoblasts Transfected to Express GFP-Lamin A Fusion Proteins

GFP-fusion protein expressed	Relative aggregate fluorescence intensity (±SE)[a]	Number of aggregates analyzed
GFP-LaA	1	80
GFP-N195K	0.81 ± 0.31	120
GFP-E358K	0.61 ± 0.02	54
GFP-M371K	0.81 ± 0.07	165
GFP-R386K	0.96 ± 0.16	104

[a]The mean nuclear fluorescence intensities (from two separate experiments where live cell imaging was performed 24 h post transfection) of mutant aggregates compared to aggregates in cells expressing GFP-LaA.

such cytoplasmic structures were not observed in cells expressing FLAG-LaAN195K alone, although diffuse cytoplasmic staining was detectable in a few cells.

Core Histones H2A and H2B Are Not Detected in Nuclear Aggregates

Previous studies have shown that lamin A binds DNA directly [Stierle et al., 2003], and is also able to bind to chromatin/polynucleosomes/core histones [Hoger et al., 1991; Yuan et al., 1991; Taniura et al., 1995] and assemble onto the surface of chromosomes [Burke, 1990; Glass and Gerace, 1990]. Although a chromatin/core histone binding region has been mapped to the C-terminal domain of LaA [Hoger et al., 1991; Taniura et al., 1995], and a binding site for mitotic chromosomes identified in the rod domain [Glass and Gerace, 1990], direct interaction with the core histones H2A and H2B has only been demonstrated in vitro for the *Drosophila* lamin Dm_o B-type lamin [Goldberg et al., 1999]. We decided to use live cell imaging to investigate whether expression of the nuclear aggregating lamin A mutants N195K and R386K would affect the subnuclear distribution of histone H2A and H2B in HeLa cells. Coexpressing GFP-LaA and DsRed2-H2A or -H2B did not result in an altered distribution of either protein (Fig. 5B). GFP-LaA localized predominantly to the nuclear rim while the DsRed2-fusion proteins displayed a uniform nucleoplasmic distribution with nucleolar exclusion, similar to cells expressing DsRed2-H2A and DsRed2-H2B alone (Fig. 5A). Interestingly, nuclear aggregate formation by GFP-LaA was not observed in double transfected cells. Despite previous reports of an interaction between the core histones H2A, H2B and lamin Dm_o, no discernible overlap in localization between

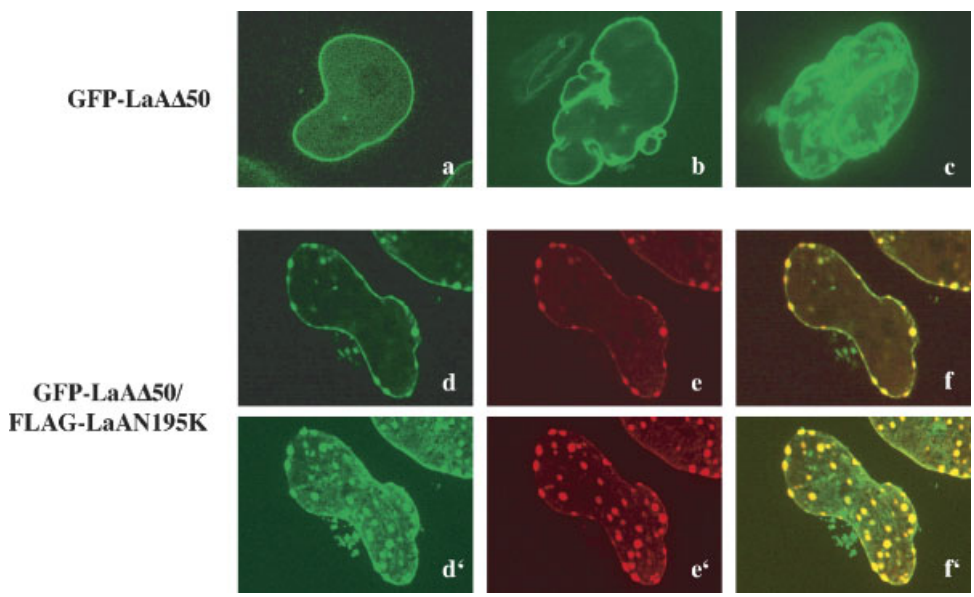

Fig. 4. Subnuclear localization of ectopically expressed GFP-LaAΔ50 in HeLa cells. The **top panel** depicts equatorial (**a**, **b**) and projection (**c**) images of living HeLa cells expressing GFP-LaAΔ50 16–24 h post transfection. Beside localization of GFP-LaAΔ50 at the nuclear envelope (**a**), its expression induces nuclear lobulations (**b**, **c**). The middle and **lower panels** show equatorial (**d**–**f**) and projection (**d′**–**f′**) images of HeLa cells coexpressing GFP-LaAΔ50 (**d** and **d′**) and FLAG-LaAN195K (**e** and **e′**). The merged images are shown in **f** and **f′**. Immunofluorescence analysis of FLAG-LaAN195K was performed 48 h post transfection on methanol/acetone fixed cells, using a rabbit FLAG-antibody and an Alexa 568-coupled secondary antibody. [Color figure can be viewed in the online issue, which is available at www.interscience.wiley.com.]

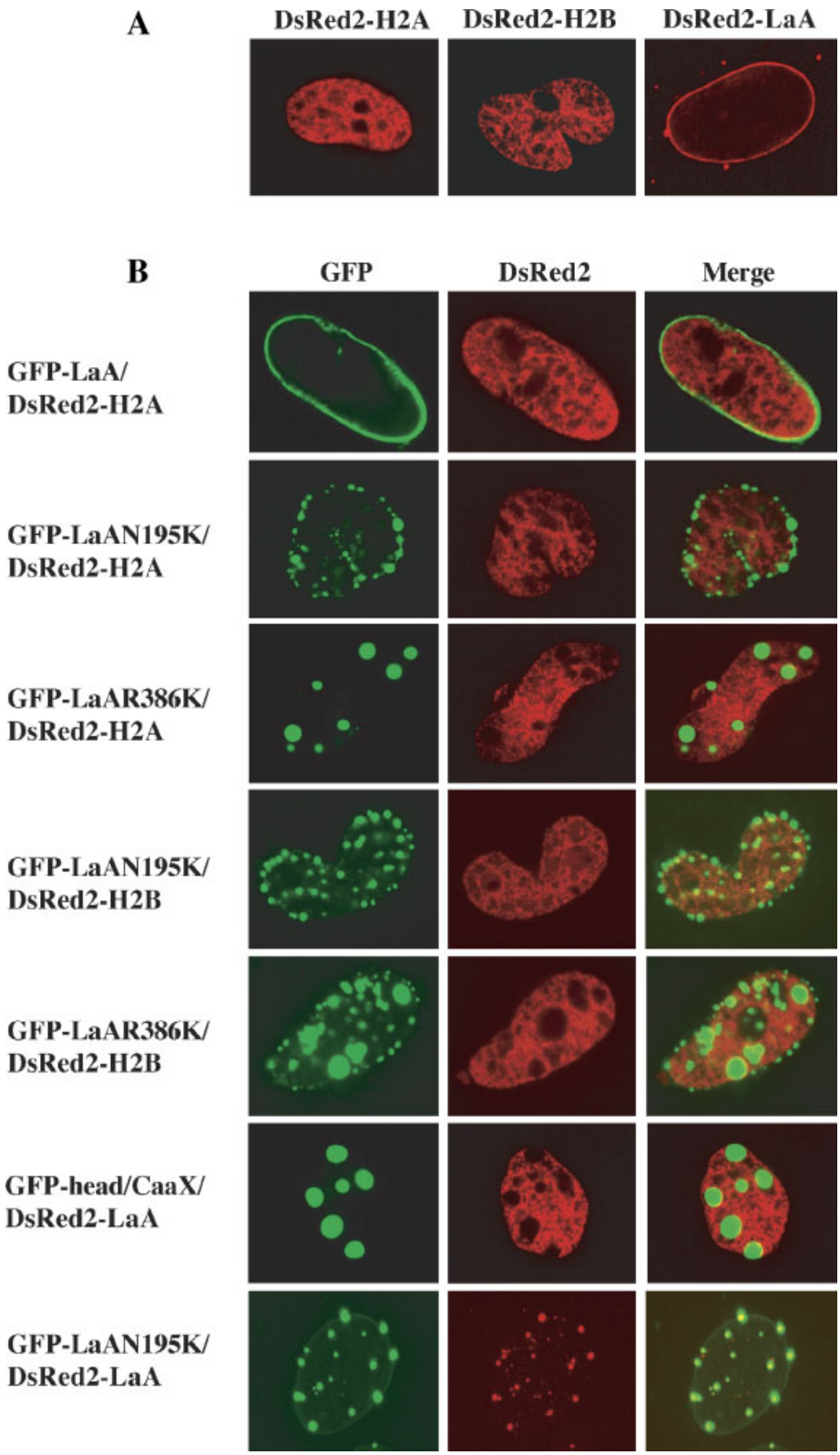

Fig. 5. Lack of colocalization of ectopically expressed histone H2A and H2B with mutant lamin A in nuclear aggregates. Live cell imaging of HeLa cells expressing DsRed2-H2A, DsRed2-H2B, and DsRed2-LaA alone (**A**) or together with the lamin A fusion proteins GFP-LaA, GFP-LaAN195K, GFP-LaAR386K, GFP-head/CaaX (**B**) 48 h post transfection. The **left panels** represent wild type and mutant GFP-lamin A fusion proteins, the **middle panels** the core histones H2A, H2B as well as LaA fused to DsRed2. Images on the right represent the merged images, where yellow coloration is indicative of colocalization. [Color figure can be viewed in the online issue, which is available at www.interscience.wiley.com.]

histones and the lamin A mutants could be detected in cells containing nuclear aggregates due to GFP-LaAN195K or GFP-LaA386K expression (Fig. 5B). This was particularily prominent in cells expressing the assembly incompetent lamin A mutant GFP-head/CaaX (Fig. 5B). Colocalization of GFP-LaAN195K and DsRed2-LaA in nuclear aggregates was observed in double transfected HeLa cells (Fig. 5B). Intriguingly nuclear aggregation of DsRed2-LaA in single transfected cells was not detected, although some cytoplasmic aggregates were observed (Fig. 5A).

Nuclear Accumulation of H2A Is Not Impaired in HeLa Cells Containing Lamin A Aggregates

To assess whether nuclear import of the core histones might be reduced in the cells overexpressing the various LaA derivatives, the mean nuclear fluorescence of DsRed2-H2A was derived by image analysis (see Materials and Methods) of CLSM files of HeLa cells expressing DsRed2-H2A with or without coexpression of GFP-LaA proteins. The results revealed strong nuclear accumulation (Fn = 22) for DsRed2-H2A alone, with the Fn values for DsRed2-H2A in cells containing nuclear aggregates of GFP-LaA, GFP-LaAN195K, and GFP-LaAR 386K not significantly different (see Table III). Similar results were obtained in cells expressing GFP-head/CaaX and GFP-LaAΔ50 (Table III). Thus, there was no effect on H2A nuclear localization elicited by the overexpression of the laminopathy-inducing lamin A mutants.

DISCUSSION

This study examines for the first time the subnuclear localization and protein recruitment properties of lamin A mutant proteins fused to GFP in living cells. The mutants used in this investigation all cause visible defects on lamin A assembly, either accumulating within nuclear aggregates, consistent with observations in fibroblasts from laminopathy patients [Capanni et al., 2003; Muchir et al., 2004], or induce highly lobulated nuclei in the case of the progerin mutant [Goldman et al., 2004]. In the context of nuclear aggregate formation and the dependence on lamin A for lamina stability [Schirmer and Gerace, 2004], mislocalization by lamin A mutants might interfere with the localization/function of lamins, as well as lamin A-binding proteins [Bechert et al., 2003]. Here we show that expression of the four-rod domain mutants, GFP-LaAN195K, -LaAE358K, -LaAM 371K, and -LaAR386K, resulted in aberrant subnuclear localization, with the formation of nuclear aggregates being the most overt nuclear phenotype. Although a similar phenotype was observed in GFP-LaA expressing cells, the tendency of nuclear aggregate formation for GFP-LaA was significantly lower compared to cells expressing the rod domain mutants (see Table I), in agreement with previous observations [Ostlund et al., 2001; Bechert et al., 2003; Holt et al., 2003]. The differences in the absolute percentage of nuclei with nuclear aggregates found in these studies, however, and those found here might be due in part to cell line differences/culture conditions and/or the SV40 promoter in pSVK3-derived constructs, which drives lower expression than the CMV promoter used here. Bechert et al. [2003] reported a time-dependent increase of cells containing nuclear aggregates; presumably the lower expression levels result in slower kinetics due to the need to achieve threshold levels for aggregate formation.

TABLE III. Summary of Results for Nuclear Accumulation of DsRed2-H2A in HeLa Cells Coexpressing Wild Type or Mutant GFP-Lamin A Proteins

Fusion proteins expressed[a]	DsRed2-H2A nuclear fluorescence intensity (mean ± SE)[b]	Number of nuclei analyzed
DsRed2-H2A	22.0 ± 0.5	41
DsRed2-H2A + GFP-LaA	23.4 ± 1.2	58
DsRed2-H2A + GFP-LaAN195K	21.3 ± 1.6	45
DsRed2-H2A + GFP-LaAR3862K	21.3 ± 1.3	45
DsRed2-H2A + GFP-LaAΔ50	27.3 ± 1.6	57
DsRed2-H2A + GFP-LaA[c]	21.6 ± 1.2	33
DsRed2-H2A + GFP-head/CaaX[c]	27.5 ± 1.8	37

[a]HeLa cells expressing DsRed2-H2A in the presence or absence of either wild type or mutant forms of human lamin A as indicated.
[b]Results represent the mean ± SE for the nuclear fluorescence intensity, determined as described in Materials and Methods. There were no significant differences between samples.
[c]Expression of respective fusion proteins from pEGFPC-derived vectors [Izumi et al. [2000].

Lamins assemble quite differently from cytoplasmic IF proteins, the first step being linear head-to-tail association of lamin dimers. The C-terminal region of coil 2B and the N-terminal part of coil 1A seem to play an important role in this process [Strelkov et al., 2004]. It thus seems reasonable to postulate that mutations within these regions may interfere with the head-to-tail assembly of A-type lamin dimers. Although the position of the acidic amino acid 358 is conserved in both vertebrate and invertebrate lamins and the mutation of a glutamic acid to a lysine residue represents a large change, aberrant subnuclear localization of the E358K mutant compared to the other rod domain mutants was found to be moderate. In contrast, residue 386, located at the very end of the rod domain, seems to play a much more important role in lamina localization, which is supported by the observation that the arginine to lysine mutation, although leading to EDMD, does not alter the charge. The M371K missense mutation, which could possibly interfere with the interactions mediated by the rod-flanking sequences, severely impacts on lamina localization in similar fashion to the R386K mutation. The head and tail domains have been shown to be an important part of general IF assembly, with the head domain absolutely necessary for linear lamin assembly [Stuurman et al., 1996; Sasse et al., 1997]. We found significantly higher nuclear aggregate formation for all of the tail mutants tested compared to the wild type molecule. The most dramatic impact on lamina localization was observed for the R482L mutant, whereas discontinous NE-fluorescence was more prominent for the G465D and R527P mutants. Intriguingly, in the case of R482L, a similar mutation, R482W, showed only a low tendency of nuclear aggregate formation, which was comparable to that of wild type lamin A [Raharjo et al., 2001]. Nuclear aggregate formation was seen, not only upon expression of mutant lamin A, but also upon expression of GFP-LaA in HeLa cells. This may be due to the inability of the lamina to compensate for the surplus of expressed lamin A molecules, comparable to aggregate formation in desminopathy patients due to overexpression of the IF protein desmin [Costa et al., 2004], or in cultured cells upon overexpression of glial fibrillary acidic protein [Koyama and Goldman, 1999]. In general, the nuclear phenotypes of cells expressing GFP lamin A mutant proteins resembled those found in previous studies where FLAG or HA-tagged lamin A mutants were analyzed. As shown previously [Bechert et al., 2003], the majority of nuclear aggregates localized at the periphery of the nucleus, but the large irregularly formed nuclear aggregates observed by others in a small population of transfected cells [Ostlund et al., 2001; Bechert et al., 2003] were not seen here. Our study clearly implies that discontinuous lamina localization and the formation of nuclear aggregates, is likely to be a disease-related molecular event (see below).

Opposed to the EDMD-, DCM,- and FPLD-causing missense mutations described above, the premature aging syndrome HGPS is caused by a lamin A in-frame deletion mutant. Immunofluorescence studies on cultured HGPS-derived cells have previously revealed structural abnormalities of the nucleus [De Sandre-Giovannoli et al., 2003; Eriksson et al., 2003; Bridger and Kill, 2004; Goldman et al., 2004], correlating with mislocalization of lamin A, increased hyperproliferation and apoptosis [Bridger and Kill, 2004]. Overexpression of GFP-LaAΔ50 in HeLa cells resulted in the formation of lobulated nuclei here, similar to the effect of microinjecting LaAΔ50 into cultured cells [Goldman et al., 2004]. Intriguingly, NE-lobulation was found to be more pronounced in pEPI-derived GFP-LaAΔ50 expressing Hela cells than in those expressing pDEST53-encoded GFP-LaAΔ50, which might be accounted for by increased expression levels (see above). We additionally observed reduced aggregate formation compared to cells expressing the wild type molecule. Formation of lobulated nuclei presumably results from constitutive farnesylation of the partially processed pre-lamin A protein, with the mutant protein possibly having effects on lamin dynamics [Goldman et al., 2005]. Coexpression studies revealed no effect on the subnuclear distribution of the core histone fusion proteins DsRed2-H2A and DsRed2-H2B in living HeLa cells containing GFP-LaAN195K or GFP-LaAR386K nuclear aggregates, in contrast to DsRed2-LaA, which was found to colocalize with nuclear aggregates.

Reported association of pathogenic A-type lamin mutant expression with nuclear architectural defects [Vigouroux et al., 2001; Novelli et al., 2002; Caux et al., 2003; Chen et al., 2003; Eriksson et al., 2003; Favreau et al., 2003;

Muchir et al., 2003], altered positioning of the NPC [Goldman et al., 2004] and the NPC component NUP153 [Bechert et al., 2003; Muchir et al., 2003; Goldman et al., 2004], a key protein in various nuclear transport pathways, do not exclude the possible interference of lamin defects on nuclear transport processes.

In this context nuclear import of SREBP1 has indeed been reported to be impaired in *LMNA*$^{-/-}$ mice [Nikolova et al., 2004], encouraging us to examine nuclear import processes for effects of the overexpression of lamin A mutants. Exploiting our different fluorescently tagged proteins, it proved possible to study subcellular localization of DsRed2-H2A in living, GFP-lamin A-mutant expressing cells. Quantitative analysis revealed that, despite the presence of nuclear aggregates or NE-lobulation, nuclear accumulation of DsRed2-H2A was not significantly different to that in cells expressing DsRed2-H2A alone. Nuclear import of core histones in mammalian cells and yeast is mediated through pathways involving several different members of the importin family [Mosammaparast et al., 2001; Muhlhausser et al., 2001], at least some of which thus appear not to be perturbed by impaired lamin A/NPC function. With the increasing availability of karyophilic fluorescently tagged proteins this issue will be able to be investigated in more detail in the future and should shed new light on the effect of mislocalizing lamin A on lamin A binding proteins and the role this may play in laminopathy pathogenesis. Importantly in this context, we have recently shown [Hübner et al., 2005] that transcriptional regulators such as Rb and SREBP-1a are recruited to lamin A-mutant-induced nuclear aggregates, supporting the idea that perturbation of gene expression (see introduction) may be a critical factor in the progression of laminopathogenesis and its apparently tissue-specific nature.

ACKNOWLEDGMENTS

We thank H. J. Worman and M. Osborn for providing human wildtype and mutant lamin A cDNA constructs and D.M. Gilbert for providing the head/CaaX lamin A mutant construct.

REFERENCES

Bechert K, Lagos-Quintana M, Harborth J, Weber K, Osborn M. 2003. Effects of expressinglamin A mutant protein causing Emery–Dreifuss muscular dystrophy and familial partial lipodystrophy in HeLa cells. Exp Cell Res 286:75–86.

Beck LA, Hosick TJ, Sinensky M. 1990. Isoprenylation is required for the processing of the lamin A precursor. J Cell Biol 110:1489–1499.

Bonne G, Di Barletta MR, Varnous S, Becane HM, Hammouda EH, Merlini L, Muntoni F, Greenberg CR, Gary F, Urtizberea JA, Duboc D, Fardeau M, Toniolo D, Schwartz K. 1999. Mutations in the gene encoding lamin A/C cause autosomal dominant Emery–Dreifuss muscular dystrophy. Nat Genet 21:285–288.

Bonne G, Mercuri E, Muchir A, Urtizberea A, Becane HM, Recan D, Merlini L, Wehnert M, Boor R, Reuner U, Vorgerd M, Wicklein EM, Eymard B, Duboc D, Penisson-Besnier I, Cuisset JM, Ferrer X, Desguerre I, Lacombe D, Bushby K, Pollitt C, Toniolo D, Fardeau M, Schwartz K, Muntoni F. 2000. Clinical and molecular genetic spectrum of autosomal dominant Emery–Dreifuss muscular dystrophy due to mutations of the lamin A/C gene. Ann Neurol 48:170–180.

Bridger JM, Kill IR. 2004. Aging of Hutchinson–Gilford progeria syndrome fibroblasts is characterised by hyperproliferation and increased apoptosis. Exp Gerontol 39:717–724.

Bridger JM, Kill IR, O'Farrell M, Hutchison CJ. 1993. Internal lamin structures within G1 nuclei of human dermal fibroblasts. J Cell Sci 104(Pt 2):297–306.

Broers JL, Peeters EA, Kuijpers HJ, Endert J, Bouten CV, Oomens CW, Baaijens FP, Ramaekers FC. 2004. Decreased mechanical stiffness in LMNA$^{-/-}$ cells is caused by defective nucleo-cytoskeletal integrity: Implications for the development of laminopathies. Hum Mol Genet 13:2567–2580.

Broers JL, Kuijpers HJ, Ostlund C, Worman HJ, Endert J, Ramaekers FC. 2005. Both lamin A and lamin C mutations cause lamina instability as well as loss of internal nuclear lamin organization. Exp Cell Res 304: 582–592.

Burke B. 1990. On the cell-free association of lamins A and C with metaphase chromosomes. Exp Cell Res 186:169–176.

Cao H, Hegele RA. 2000. Nuclear lamin A/C R482Q mutation in canadian kindreds with Dunnigan-type familial partial lipodystrophy. Hum Mol Genet 9:109–112.

Cao H, Hegele RA. 2003. LMNA is mutated in Hutchinson–Gilford progeria, (MIM 176670) but not in Wiedemann-Rautenstrauch progeroid syndrome (MIM 264090). J Hum Genet 48:271–274.

Capanni C, Cenni V, Mattioli E, Sabatelli P, Ognibene A, Columbaro M, Parnaik VK, Wehnert M, Maraldi NM, Squarzoni S, Lattanzi G. 2003. Failure of lamin A/C to functionally assemble in R482L mutated familial partial lipodystrophy fibroblasts: Altered intermolecular interaction with emerin and implications for gene transcription. Exp Cell Res 291:122–134.

Caux F, Dubosclard E, Lascols O, Buendia B, Chazouilleres O, Cohen A, Courvalin JC, Laroche L, Capeau J, Vigouroux C, Christin-Maitre S. 2003. A new clinical condition linked to a novel mutation in lamins A and C with generalized lipoatrophy, insulin-resistant diabetes, disseminated leukomelanodermic papules, liver steatosis, and cardiomyopathy. J Clin Endocrinol Metab 88: 1006–1013.

Chen L, Lee L, Kudlow BA, Dos Santos HG, Sletvold O, Shafeghati Y, Botha EG, Garg A, Hanson NB, Martin GM, Mian IS, Kennedy BK, Oshima J. 2003. LMNA mutations in atypical Werner's syndrome. Lancet 362: 440–445.

Costa ML, Escaleira R, Cataldo A, Oliveira F, Mermelstein CS. 2004. Desmin: Molecular interactions and putative functions of the muscle intermediate filament protein. Braz J Med Biol Res 37:1819–1830.

De Sandre-Giovannoli A, Bernard R, Cau P, Navarro C, Amiel J, Boccaccio I, Lyonnet S, Stewart CL, Munnich A, Le Merrer M, Levy N. 2003. Lamin a truncation in Hutchinson–Gilford progeria. Science 300:2055.

Dhe-Paganon S, Werner ED, Chi YI, Shoelson SE. 2002. Structure of the globular tail of nuclear lamin. J Biol Chem 277:17381–17384.

Dreuillet C, Tillit J, Kress M, Ernoult-Lange M. 2002. In vivo and in vitro interaction between human transcription factor MOK2 and nuclear lamin A/C. Nucleic Acids Res 30:4634–4642.

Eriksson M, Brown WT, Gordon LB, Glynn MW, Singer J, Scott L, Erdos MR, Robbins CM, Moses TY, Berglund P, Dutra A, Pak E, Durkin S, Csoka AB, Boehnke M, Glover TW, Collins FS. 2003. Recurrent de novo point mutations in lamin A cause Hutchinson–Gilford progeria syndrome. Nature 423:293–298.

Fatkin D, MacRae C, Sasaki T, Wolff MR, Porcu M, Frenneaux M, Atherton J, Vidaillet HJ, Jr., Spudich S, De Girolami U, Seidman JG, Seidman C, Muntoni F, Muehle G, Johnson W, McDonough B. 1999. Missense mutations in the rod domain of the lamin A/C gene as causes of dilated cardiomyopathy and conduction-system disease. N Engl J Med 341:1715–1724.

Favreau C, Dubosclard E, Ostlund C, Vigouroux C, Capeau J, Wehnert M, Higuet D, Worman HJ, Courvalin JC, Buendia B. 2003. Expression of lamin A mutated in the carboxyl-terminal tail generates an aberrant nuclear phenotype similar to that observed in cells from patients with Dunnigan-type partial lipodystrophy and Emery–Dreifuss muscular dystrophy. Exp Cell Res 282:14–23.

Forwood JK, Jans DA. 2002. Nuclear import pathway of the telomere elongation suppressor TRF1: Inhibition by importin alpha. Biochemistry 41:9333–9340.

Ghildyal R, Ho A, Wagstaff KM, Dias MD, Barton CL, Jans P, Bardin P, Jans DA. 2005. Nuclear import of the respiratory syncytial virus matrix protein is mediated by importin1 independent of importin. Biochemistry 44: 12887–12895.

Gilchrist S, Gilbert N, Perry P, Ostlund C, Worman HJ, Bickmore WA. 2004. Altered protein dynamics of disease-associated lamin A mutants. BMC Cell Biol 5:46.

Glass JR, Gerace L. 1990. Lamins A and C bind and assemble at the surface of mitotic chromosomes. J Cell Biol 111:1047–1057.

Goldberg M, Harel A, Brandeis M, Rechsteiner T, Richmond TJ, Weiss AM, Gruenbaum Y. 1999. The tail domain of lamin Dmo binds histones H2A and H2B. Proc Natl Acad Sci USA 96:2852–2857.

Goldman RD, Shumaker DK, Erdos MR, Eriksson M, Goldman AE, Gordon LB, Gruenbaum Y, Khuon S, Mendez M, Varga R, Collins FS. 2004. Accumulation of mutant lamin A causes progressive changes in nuclear architecture in Hutchinson–Gilford progeria syndrome. Proc Natl Acad Sci USA 101:8963–8968.

Goldman RD, Goldman AE, Shumaker DK. 2005. Nuclear lamins: Building blocks of nuclear structure and function. Novartis Found Symp 264:3–16; discussion 16–21, 227–230.

Hoger TH, Krohne G, Kleinschmidt JA. 1991. Interaction of Xenopus lamins A and LII with chromatin in vitro mediated by a sequence element in the carboxyterminal domain. Exp Cell Res 197:280–289.

Holt I, Clements L, Manilal S, Brown SC, Morris GE. 2001. The R482Q lamin A/C mutation that causes lipodystrophy does not prevent nuclear targeting of lamin A in adipocytes or its interaction with emerin. Eur J Hum Genet 9:204–208.

Holt I, Ostlund C, Stewart CL, Man N, Worman HJ, Morris GE. 2003. Effect of pathogenic missense mutations in lamin A on its interaction with emerin in vivo. J Cell Sci 116:3027–3035.

Hozak P, Sasseville AM, Raymond Y, Cook PR. 1995. Lamin proteins form an internal nucleoskeleton as well as a peripheral lamina in human cells. J Cell Sci 108(Pt 2): 635–644.

Hu W, Jans DA. 1999. Efficiency of importin alpha/beta-mediated nuclear localization sequence recognition and nuclear import. Differential role of NTF2. J Biol Chem 274:15820–15827.

Hübner S, Eam JE, Hübner A, Jans DA. 2006. Laminopathy-inducing lamin A mutants can induce redistribution of lamin binding proteins into nuclear aggregates. Exp Cell Res 312:171–183.

Izumi M, Vaughan OA, Hutchison CJ, Gilbert DM. 2000. Head and/or CaaX domain deletions of lamin proteins disrupt preformed lamin A and C but not lamin B structure in mammalian cells. Mol Biol Cell 11:4323–4337.

Jagatheesan G, Thanumalayan S, Muralikrishna B, Rangaraj N, Karande AA, Parnaik VK. 1999. Colocalization of intranuclear lamin foci with RNA splicing factors. J Cell Sci 112(Pt24):4651–4661.

Kennedy BK, Barbie DA, Classon M, Dyson N, Harlow E. 2000. Nuclear organization of DNA replication in primary mammalian cells. Genes Dev 14:2855–2868.

Koyama Y, Goldman JE. 1999. Formation of GFAP cytoplasmic inclusions in astrocytes and their disaggregation by alpha B-crystallin. Am J Pathol 154:1563–1572.

Krimm I, Ostlund C, Gilquin B, Couprie J, Hossenlopp P, Mornon JP, Bonne G, Courvalin JC, Worman HJ, Zinn-Justin S. 2002. The Ig-like structure of the C-terminal domain of laminA/C, mutated in muscular dystrophies, cardiomyopathy, and partial lipodystrophy. Structure (Camb) 10:811–823.

Lammerding J, Schulze PC, Takahashi T, Kozlov S, Sullivan T, Kamm RD, Stewart CL, Lee RT. 2004. Lamin A/C deficiency causes defective nuclear mechanics and mechanotransduction. J Clin Invest 113:370–378.

Lenz-Bohme B, Wismar J, Fuchs S, Reifegerste R, Buchner E, Betz H, Schmitt B. 1997. Insertional mutation of the *Drosophila* nuclear lamin *Dmo* gene results in defective nuclear envelopes, clustering of nuclear pore complexes, and accumulation of annulate lamellae. J Cell Biol 137: 1001–1016.

Liu J, Ben-Shahar TR, Riemer D, Treinin M, Spann P, Weber K, Fire A, Gruenbaum Y. 2000. Essential roles for Caenorhabditis elegans lamin gene in nuclear organization,

cell cycle progression, and spatial organization of nuclear pore complexes. Mol Biol Cell 11:3937–3947.

Lloyd DJ, Trembath RC, Shackleton S. 2002. A novel interaction between lamin A and SREBP1: Implications for partial lipodystrophy and other laminopathies. Hum Mol Genet 11:769–777.

Machiels BM, Broers JL, Raymond Y, de Ley L, Kuijpers HJ, Caberg NE, Ramaekers FC. 1995. Abnormal A-type lamin organization in a human lung carcinoma cell line. Eur J Cell Biol 67:328–335.

Markiewicz E, Dechat T, Foisner R, Quinlan RA, Hutchison CJ. 2002a. Lamin A/C binding protein LAP2alpha is required for nuclear anchorage of retinoblastoma protein. Mol Biol Cell 13:4401–4413.

Markiewicz E, Venables R, Mauricio Alvarez R, Quinlan R, Dorobek M, Hausmanowa-Petrucewicz I, Hutchison C. 2002b. Increased solubility of lamins and redistribution of lamin C in X-linked Emery–Dreifuss muscular dystrophy fibroblasts. J Struct Biol 140:241–253.

Moir RD, Montag-Lowy M, Goldman RD. 1994. Dynamic properties of nuclear lamins: Lamin B is associated with sites of DNA replication. J Cell Biol 125:1201–1212.

Mosammaparast N, Jackson KR, Guo Y, Brame CJ, Shabanowitz J, Hunt DF, Pemberton LF. 2001. Nuclear import of histone H2A and H2B is mediated by a network of karyopherins. J Cell Biol 153:251–262.

Muchir A, van Engelen BG, Lammens M, Mislow JM, McNally E, Schwartz K, Bonne G. 2003. Nuclear envelope alterations in fibroblasts from LGMD1B patients carrying nonsense Y259X heterozygous or homozygous mutation in lamin A/C gene. Exp Cell Res 291:352–362.

Muchir A, Medioni J, Laluc M, Massart C, Arimura T, van der Kooi AJ, Desguerre I, Mayer M, Ferrer X, Briault S, Hirano M, Worman HJ, Mallet A, Wehnert M, Schwartz K, Bonne G. 2004. Nuclear envelope alterations in fibroblasts from patients with muscular dystrophy, cardiomyopathy, and partial lipodystrophy carrying lamin A/C gene mutations. Muscle Nerve 30:444–450.

Muhlhausser P, Muller EC, Otto A, Kutay U. 2001. Multiple pathways contribute to nuclear import of core histones. EMBO Rep 2:690–696.

Muralikrishna B, Thanumalayan S, Jagatheesan G, Rangaraj N, Karande AA, Parnaik VK. 2004. Immunolocalization of detergent-susceptible nucleoplasmic lamin A/C foci by a novel monoclonal antibody. J Cell Biochem 91:730–739.

Neri LM, Raymond Y, Giordano A, Borgatti P, Marchisio M, Capitani S, Martelli AM. 1999. Spatial distribution of lamin A and B1 in the K562 cell nuclear matrix stabilized with metal ions. J Cell Biochem 75:36–45.

Newport JW, Wilson KL, Dunphy WG. 1990. A lamin-independent pathway for nuclear envelope assembly. J Cell Biol 111:2247–2259.

Nikolova V, Leimena C, McMahon AC, Tan JC, Chandar S, Jogia D, Kesteven SH, Michalicek J, Otway R, Verheyen F, Rainer S, Stewart CL, Martin D, Feneley MP, Fatkin D. 2004. Defects in nuclear structure and function promote dilated cardiomyopathy in lamin A/C deficient mice. J Clin Invest 113:357–369.

Novelli G, Muchir A, Sangiuolo F, Helbling-Leclerc A, D'Apice MR, Massart C, Capon F, Sbraccia P, Federici M, Lauro R, Tudisco C, Pallotta R, Scarano G, Dallapiccola B, Merlini L, Bonne G. 2002. Mandibuloacral dysplasia is caused by a mutation in LMNA-encoding lamin A/C. Am J Hum Genet 71:426–431.

Ostlund C, Bonne G, Schwartz K, Worman HJ. 2001. Properties of lamin A mutants found in Emery–Dreifuss muscular dystrophy, cardiomyopathy and Dunnigan-type partiall lipodystrophy. J Cell Sci 114:4435–4445.

Ozaki T, Saijo M, Murakami K, Enomoto H, Taya Y, Sakiyama S. 1994. Complex formation between lamin A and the retinoblastoma gene product: Identification of the domain on laminA required for its interaction. Oncogene 9:2649–2653.

Piechaczek C, Fetzer C, Baiker A, Bode J, Lipps HJ. 1999. A vector based on the SV40 origin of replication and chromosomal S/MARs replicates episomally in CHO cells. Nucleic Acids Res 27:426–428.

Pugh GE, Coates PJ, Lane EB, Raymond Y, Quinlan RA. 1997. Distinct nuclear assembly pathways for lamins A and C lead to their increase during quiescence in Swiss 3T3 cells. J Cell Sci 110(Pt 19):2483–2493.

Raharjo WH, Enarson P, Sullivan T, Stewart CL, Burke B. 2001. Nuclear envelope defects associated with LMNA mutations cause dilated cardiomyopathy and Emery–Dreifuss muscular dystrophy. J Cell Sci 114:4447–4457.

Sasse B, Lustig A, Aebi U, Stuurman N. 1997. In vitro assembly of *Drosophila* lamin *Dmo*–lamin polymerization properties are conserved. Eur J Biochem 250:30–38.

Sasseville AM, Raymond Y. 1995. Lamin A precursor is localized to intranuclear foci. J Cell Sci 108(Pt 1):273–285.

Schirmer EC, Gerace L. 2004. The stability of the nuclear lamina polymer changes with the composition of lamin subtypes according to their individual binding strengths. J Biol Chem 279:42811–42817.

Sebillon P, Bouchier C, Bidot LD, Bonne G, Ahamed K, Charron P, Drouin-Garraud V, Millaire A, Desrumeaux G, Benaiche A, Charniot JC, Schwartz K, Villard E, Komajda M. 2003. Expanding the phenotype of LMNA mutations in dilated cardiomyopathy and functional consequences of these mutations. J Med Genet 40:560–567.

Shackleton S, Lloyd DJ, Jackson SN, Evans R, Niermeijer MF, Singh BM, Schmidt H, Brabant G, Kumar S, Durrington PN, Gregory S, O'Rahilly S, Trembath RC. 2000. LMNA, encoding lamin A/C, is mutated in partial lipodystrophy. Nat Genet 24:153–156.

Sinensky M, Fantle K, Trujillo M, McLain T, Kupfer A, Dalton M. 1994a. The processing pathway of prelamin A. J Cell Sci 107(Pt 1):61–67.

Sinensky M, McLain T, Fantle K. 1994b. Expression of prelamin A but not mature lamin A confers sensitivity of DNA biosynthesis to lovastatin on F9 teratocarcinoma cells. J Cell Sci 107(Pt 8):2215–2218.

Soboleva TA, Jans DA, Johnson-Saliba M, Baker RT. 2005. Nuclear-cytoplasmic shuttling of the oncogenic mouse UNP/USP4 deubiquitylating enzyme. J Biol Chem 280: 745–752.

Spann TP, Moir RD, Goldman AE, Stick R, Goldman RD. 1997. Disruption of nuclear lamin organization alters the distribution of replication factors and inhibits DNA synthesis. J Cell Biol 136:1201–1212.

Stierle V, Couprie J, Ostlund C, Krimm I, Zinn-Justin S, Hossenlopp P, Worman HJ, Courvalin JC, Duband-Goulet I. 2003. The carboxyl-terminal region common to

lamins A and C contains a DNA binding domain. Biochemistry 42:4819–4828.

Strelkov SV, Schumacher J, Burkhard P, Aebi U, Herrmann H. 2004. Crystal structure of the human lamin A coil 2B dimer: Implications for the head-to-tail association of nuclear lamins. J Mol Biol 343:1067–1080.

Stuurman N, Sasse B, Fisher PA. 1996. Intermediate filament protein polymerization: Molecular analysis of *Drosophila* nuclear lamin head-to-tail binding. J Struct Biol 117:1–15.

Sullivan T, Escalante-Alcalde D, Bhatt H, Anver M, Bhat N, Nagashima K, Stewart CL, Burke B. 1999. Loss of A-type lamin expression compromises nuclear envelope integrity leading to muscular dystrophy. J Cell Biol 147: 913–920.

Taniura H, Glass C, Gerace L. 1995. A chromatin binding site in the tail domain of nuclear lamins that interacts with core histones. J Cell Biol 131:33–44.

Vigouroux C, Auclair M, Dubosclard E, Pouchelet M, Capeau J, Courvalin JC, Buendia B. 2001. Nuclear envelope disorganization in fibroblasts from lipodystrophic patients with heterozygous R482Q/W mutations in the lamin A/C gene. J Cell Sci 114:4459–4468.

Weber K, Plessmann U, Traub P. 1989. Maturation of nuclear lamin A involves a specific carboxy-terminal trimming, which removes the polyisoprenylation site from the precursor; implications for the structure of the nuclear lamina. FEBS Lett 257:411–414.

Yuan J, Simos G, Blobel G, Georgatos SD. 1991. Binding of lamin A to polynucleosomes. J Biol Chem 266:9211–9215.